

# The origin of the allometric scaling of lung's ventilation in mammals

Frédérique Noël,<sup>1</sup> Cyril Karamaoun,<sup>1</sup> and Benjamin Mauroy<sup>1</sup>

<sup>1</sup>*Université Côte d'Azur, CNRS, LJAD, Vader center, Nice, France*

(Dated: September 15, 2022)

A model of optimal control of ventilation recently developed for humans has suggested that the localization of the transition between a convective and a diffusive transport of the respiratory gas determines how ventilation should be controlled to minimize its energetic cost at any metabolic regime. We generalized this model to any mammal, based on the core morphometric characteristics shared by all mammals' lungs and on their allometric scaling from the literature. Since the main energetic costs of ventilation are related to the convective transport, we prove that, for all mammals, the localization of the shift from a convective transport into a diffusive transport plays a critical role on keeping that cost low while fulfilling the lung's function. Our model predicts for the first time where this transition zone should occur in order to minimize the energetic cost of ventilation, depending on the mammals' mass and on the metabolic regime. From that optimal localization, we are able to derive predicted allometric scaling laws for both tidal volumes and breathing rates, at any metabolic regime. We ran our model for the three common metabolic rates – basal, field and maximal – and showed that our predictions accurately reproduce the experimental data available in the literature. Our analysis supports the hypothesis that the mammals' allometric scaling laws of tidal volumes and breathing rates are driven by a few core geometrical characteristics shared by the mammals' lungs, the physical processes of respiratory gas transport and the metabolic needs.

In animals, the main molecular source of energy, the adenosine triphosphate (ATP), is produced through a long and intricate chain of biochemical reactions that, in fine, aims at recovering the chemical energy stored in primary energy sources, such as glucose. This energy conversion occurs mainly through oxidative processes collectively grouped under the term of cellular respiration. Glucose oxidation requires oxygen to be brought from the atmosphere through the tissues to each individual cell. Various evolutive strategies have emerged over time, from the gills of fish to the respiratory tracheae of arthropods. The mammal's lung has been selected and shaped by evolutive processes to fulfill the body needs in oxygen and to eliminate the carbon dioxide, a major by-product of cellular respiration. Thus, the architecture of this organ has evolved following the needs for gas exchange.

In mammals, the lung is composed of two major parts: the bronchial tree and the alveolar zone. The bronchial tree is structured as a nearly dichotomous tree structure wherein the airflow circulates to and from the alveolar zone, depending on the ventilation phase, i.e. inspiration or expiration. At inspiration, fresh air is brought into the alveolar region where oxygen exchange takes place by diffusion from the alveoli to the pulmonary blood circulation, through the alveolar–capillary membrane. It allows erythrocytes to be reloaded in oxygen. In parallel, the carbon dioxide by-product is transferred from the blood stream to the alveoli. Then, at expiration, a higher carbon dioxide/lower oxygen air is expelled from the lung until fresh air comes in again at the next inspiration [41].

The thin alveolar gas exchange membrane is combined with a large alveolar surface in connection to a compact bronchial tree. These characteristics have been selected by evolution to fulfill the gas exchange requirements in mammals while satisfying the structural body

needs, namely a compact and rib-covered thorax cavity [24].

The transport of air in the lung, especially in the bronchial tree, requires a certain amount of energy due to physical constraints. A hydrodynamic resistance to the air flow in the bronchi arises from friction effects, mainly due to air viscosity [21]. In parallel, mechanical energy is needed to expand the thoracic cage and the lung tissues during inspiration. That energy is lost at expiration by the viscoelastic recoil of the tissues. Without careful regulation, the amount of energy induced by these physical constraints of ventilation might correspond to a high metabolic cost, even at rest [28]. However, natural selection favors configurations that require low amounts or minima of energy. Moreover, the process of optimization by evolution is performed under the constraint of the lung's function: the gas exchange requirements have to fit the metabolism activity.

The typical functional constraint associated to that energy cost was up to recently based on the total air flow rate entering the lung only [18, 25, 28], without accounting for the gas transport in the organ. More recently, Noël & Mauroy [27] optimized the energy spent for ventilation in humans with a more realistic functional constraint, based on the oxygen flow in the alveoli, including the physics of oxygen and carbon dioxide transport in a symmetric branched model of the lung. This approach was not only able to predict physiological ventilation parameters for a wide range of metabolic regimes, but it also gave highlights on the distribution and transport of oxygen and carbon dioxide in the lung.

Actually, the progression of air in the lung is a combination of two mass transport processes: convection and diffusion. In the upper and central part of the bronchial tree, the convective transport largely dominates the mass

transport, driven by the pressure gradient imposed by the airflow. However, as the cumulative surface of the bronchi section area increases at each bifurcation, the air velocity decreases while progressing towards the distal part of the tree. At some point, the characteristic velocity of convection equilibrates with, and even becomes smaller than the characteristic velocity of diffusion; the mass transport becomes dominated by the diffusion process. The localization of the transition zone between convection and diffusion depends on the geometry of the lung and on the ventilation parameters. The previous work of Noël & Mauroy showed that the control of ventilation in humans localizes the transition zone as a trade-off between the oxygen demand and the availability and accessibility of the exchange surface deeper in the lung [27, 31].

The lungs of mammals share morphological and functional properties, raising the question on whether the previous results for human can be extended or not to all mammals. These shared properties are known to depend on the mass  $M$  of the animal with non trivial power laws, called allometric scaling laws [10, 15, 17, 29, 40]. The physics of ventilation, and hence its control, is linked to the geometry of the lung. Consequently, the morphological differences amongst mammals also affect the control of ventilation. This is confirmed by the allometric scaling laws followed by the ventilation frequency and tidal volume. Breathing rate at basal metabolic rate (BMR) has been estimated to follow the law  $f_b^{\text{BMR}} \simeq 0.58 M^{-\frac{1}{4}} \text{ Hz}$  [42] and tidal volume to follow the law  $V_T^{\text{BMR}} \simeq 7.14 10^{-3} M^1 \text{ L}$  [13, 40]. At other metabolic rates, less data is available in the literature except for the breathing rate of mammals at maximal metabolic rate (MMR), estimated to follow the law  $f_b^{\text{MMR}} \simeq 5.08 M^{-0.14} \text{ Hz}$  [2]. Whether or not these allometric scaling laws are reflecting the optimization throughout the whole class of mammals of the energy spent for ventilation remains still to be uncovered. A model able to predict these laws for mammals would be a powerful tool to derive them at other regimes, such as at submaximal exercise, at maximal exercise or at the field metabolic rate (FMR).

In this work, we develop two mathematical models: one to estimate the amount of oxygen captured from ambient air by idealised mammals' lungs; and one to estimate the energetic cost of ventilation. These two models depend on the mammals' mass and are coupled together to form a mathematical model for the natural selection of breathing rates and tidal volumes. Under our models' hypotheses, our analysis shows that the physiological allometric scaling laws reported in the literature for both breathing rates and tidal volumes are actually minimizing the mechanical energy of breathing. Moreover, we show that the selected configurations are mainly driven by the geometries of the mammals' lungs and by the physical processes involved in oxygen transport in the lung.

## MODELLING

### Ventilation pattern and energy cost of ventilation

Airflow velocity can be idealized by a sinusoidal pattern in time, i.e. under the form  $u_0(t) = U \sin(2\pi t/T)$ . The quantity  $U$  is the maximal velocity amplitude and  $T$  is the period of ventilation, inverse of the breathing frequency  $f_b = 1/T$ . Denoting  $S_0$  the surface area of the tracheal cross-section, the tidal volume is then  $V_T = \int_0^{\frac{T}{2}} S_0 u_0(s) ds = \frac{US_0T}{\pi}$ . The parameterization using  $(U, T)$  or  $(V_T, f_b)$  are equivalent. The flow rate is then  $\dot{V}_E = V_T f_b$ .

The biomechanics of lung's ventilation involves two active physical phenomena that are sources of an energy cost [18, 27]. First, the motion of the tissues out of their equilibrium position implies that the diaphragm has to use, during inspiration, an amount of energy that is stored in the tissues as elastic energy. This energy is then used during expiration for a passive tissues recoil. The power spent  $\mathcal{P}_e(U, T)$  is related to the elastic properties of the thoracic cage and of the lung. These properties depends on the lung's compliance  $C$  [1] which is defined as the ratio between the change in volume of the lung and the change in pleural pressure. Then,

$$\mathcal{P}_e(U, T) = \frac{1}{T} \int_0^{\frac{T}{2}} \frac{1}{C} V(t) \frac{dV}{dt}(t) = \frac{1}{C} \frac{U^2 S_0^2 T}{2\pi^2},$$

where  $V(t) = \int_0^t S_0 u_0(s) ds$  is the volume of the lung as a function of time. Second, the airflow inside the bronchi induces an energy loss due to viscous effects that has to be compensated by the motion of the diaphragm during inspiration. The viscous power dissipated depends on the hydrodynamic resistance of the lung  $R$ ,

$$\mathcal{P}_v(U, T) = \frac{1}{T} \int_0^{\frac{T}{2}} R u_0^2(t) S_0^2 ds = R \frac{U^2 S_0^2}{4},$$

The total power spent is the sum of the power spent for the displacement of the tissues and for compensating viscous effects due to air motion in the bronchi,

$$\begin{aligned} \mathcal{P}(U, T) &= \mathcal{P}_e(U, T) + \mathcal{P}_v(U, T) \\ &= \mathcal{P}_e(U, T) \left( 1 + \frac{\pi^2}{2T} RC \right) = \frac{U^2 S_0^2 T}{2\pi^2 C} \left( 1 + \frac{\pi^2}{2T} RC \right). \end{aligned} \quad (1)$$

The power can also be expressed using the equivalent ventilation parameters  $(V_T, f_b)$ ,  $\tilde{\mathcal{P}}(V_T, f_b) = \frac{V_T^2 f_b}{2C} (1 + \pi^2 f_b RC/2)$ .

The total power depends on the compliance of the lung  $C \propto M^1$  [34] and on the hydrodynamic resistance of the lung  $R \propto M^{-\frac{3}{4}}$  [40]. These two allometric scaling laws allow to search for a minimum of the total power for each

mammals' species, and to analyze the dependence of the minima on the mass.

The function  $(U, T) \rightarrow \mathcal{P}(U, T)$  is to be minimized relatively to the ventilation amplitude  $U$  and the period  $T$  with the constraint  $f_{O_2}(U, T) = \dot{V}_{O_2}$ , where  $f_{O_2}(U, T)$  is the oxygen flow resulting from a ventilation with characteristics  $(U, T)$  and  $\dot{V}_{O_2}$  the desired flow. The desired oxygen flow  $\dot{V}_{O_2}$  depends on the metabolic regime. Allometric scaling laws have been derived for basal metabolic rate,  $\dot{V}_{O_2}^{\text{BMR}} \propto M^{\frac{3}{4}}$  [20, 29], field metabolic rate  $\dot{V}_{O_2}^{\text{FMR}} \propto M^{0.64}$  [16] and maximal metabolic rate  $\dot{V}_{O_2}^{\text{max}} \propto M^{\frac{7}{8}}$  [39]. Our analysis is based on these scalings that allow to set the desired oxygen flow  $\dot{V}_{O_2}$  depending on the animal's mass. In the following, we develop a model of the lung of a mammal with mass  $M$  in order to estimate the oxygen flow  $f_{O_2}(U, T)$  that results from the ventilation of its lung with a ventilation amplitude  $U$  and a period  $T$ .

### Core properties of the geometry of the mammals' lung

The derivation of the allometric properties of ventilation is based on the previous model developed by Noël & Mauroy in [27], which is adapted to all mammals over 5 orders of magnitude in mass. Mammal's lung shares invariant characteristics [38]. First the lung has a tree-like structure with bifurcating branches. It decomposes into two parts: the bronchial tree that transports, mainly by convection, the (de)oxygenated air up and down the lung, and the acini where gas exchanges with blood occur through the alveolar–capillary membrane. The bronchial tree can be considered as auto-similar, as the size of the branches is decreasing at each bifurcation with a ratio in the whole tree close to  $h = (\frac{1}{2})^{\frac{1}{3}}$  [19, 24, 38]. In the acini, the size of the branches are considered invariant at bifurcations [35, 38].

Thus, the bronchial tree can be modelled as a tree with symmetric bifurcations [24]. A generation of the tree corresponds to the set of branches with the same number of bifurcations up to the trachea. The bronchial tree is modelled by the  $G$  first generations and the acini, where the exchanges with blood are taking place, are modelled with the  $H$  last generations [38]. The total number of generations of the tree is  $N = G + H$ . Hence, if the radius and length of the trachea are  $r_0$  and  $l_0$ , the radius  $r_i$  and length  $l_i$  of a bronchus in generation  $i$  is

$$r_i = r_0 h^i \quad (i = 0 \dots G), \quad r_i = r_G \quad (i = G + 1 \dots N) \text{ and} \\ l_i = l_0 h^i \quad (i = 0 \dots G), \quad l_i = l_G \quad (i = G + 1 \dots N).$$

The quantity  $S_i = \pi r_i^2$  is the cross-section surface area of a branch in generation  $i$ . In the bronchial tree ( $i = 0 \dots G$ ),  $S_i = h^{2i} S_0$ , while in the acini ( $i = G + 1 \dots N$ ),  $S_i = S_G$ . As air is assumed incompressible in the lung in normal

ventilation conditions [7], flow conservation leads to

$$\begin{cases} u_i = \left(\frac{1}{2h^2}\right)^i u_0 \quad (i = 0 \dots G), \\ u_i = \left(\frac{1}{2}\right)^{i-G} u_G \quad (i = G + 1 \dots N). \end{cases}$$

The derivation of a lung model that depends only on the mass requires to relate explicitly the morphological parameters involved in our model with the mass of the animal. We based our hypotheses on the datasets available in [40], which brought a large set of theoretical allometric scaling laws for the cardiorespiratory system, compatible with the ecological observations. The morphological parameters used by our model are the trachea radius  $r_0$ , the reduced trachea length  $l_0$  and the generations number  $G$  for the bronchial tree and  $H$  for the acini.

From [40],  $r_0 = aM^{\frac{3}{8}}$ . The bronchi diameters, and consequently the dead volume, are affected by the ventilation regime [5]. Since all bronchi diameters in our model are computed from the tracheal diameter, the value of the prefactor  $a$  depends on the regime and it is determined based on human data and dead volumes:  $a = 1.83 \cdot 10^{-3}$  m at BMR,  $a = 1.93 \cdot 10^{-3}$  m at FMR and  $a = 2.34 \cdot 10^{-3}$  m at MMR. The effect of exercise on the hydrodynamic resistance of the lung,  $R$ , is difficult to evaluate since exercise increases both inertia and turbulence, which tends to increase energy dissipation due to air motion in the bronchi [23]. In the absence of a relevant evaluation of the balance between the changes in geometry and the more complex fluid dynamics, we kept the same value for  $R$  whatever the regime. Nevertheless, we studied how the predictions of our model were affected by an increase or a decrease of  $R$ .

The allometric scaling law for the tracheal length can be derived from [40]. Indeed the dead volume ( $V_{\text{dead}} \propto M^1$ ) is assumed to be proportional to the tracheal volume [36]. The relationship  $V_{\text{dead}} \propto \pi r_0^2 l_0 \propto M^1$  leads to  $l_0 \propto M^{\frac{1}{4}}$ .

The computation of  $G$  and  $H$  requires to assume that the radius of alveolar ducts are similar to the radius  $r_A$  of the alveoli [38], for which an allometric scaling law is known,  $r_A \propto M^{\frac{1}{12}}$  [40]. The number of generations  $G$  of the bronchial tree is then obtained from  $r_A = r_G = r_0 h^G$ , and the number of terminal bronchioles follows  $2^G \propto M^{\frac{7}{8}}$ . This last allometric scaling law can be rewritten in the form  $G = \left[ \frac{\log(r_A/r_0)}{\log(h)} \right] = \left[ \frac{7 \log(M)}{8 \log(2)} + \text{cst} \right]$ .

The total lung's gas exchange surface  $S_A \propto M^{\frac{11}{12}}$  [40] is distributed over the walls of the alveolar ducts. A single alveolar duct has a lateral surface  $s_{\text{ad}} = 2\pi r_A l_A$  with  $l_A = l_0 h^G \propto M^{-\frac{1}{24}}$ , hence  $s_{\text{ad}} \propto M^{\frac{1}{24}}$ . The total surface of alveolar ducts in the idealised lung is then  $S_{\text{ad}} = 2^{G+1} \sum_{k=0}^{H-1} 2^k s_{\text{ad}} = 2^{G+1} (2^H - 1) s_{\text{ad}} \propto M^{\frac{11}{12}}$ . Hence, the amount of exchange surface per unit of alveolar duct surface,  $\rho_s = S_A/S_{\text{ad}}$  is such that the product  $\rho_s (2^H - 1) \propto M^0$  is independent on the mass of

Variables	Exponent		Prefactor
	Predicted [40]	Observed	
$V_L$ : Lung volume	1	1.06 [34]	53.5 mL [34]
$r_0$ : Tracheal radius	3/8	0.39 [36]	1.83 mm*
$l_0$ : Tracheal length	1/4	0.27 [36]	1.87 cm*
Morphometry	$r_A$ : Radius of alveolar ducts	1/12	0.13 [37]
	$l_A$ : Length of alveolar ducts	-1/24	N.D.
	$n_A$ : Number of alveoli	3/4	N.D.
	$v_A$ : Volume of alveolus	1/4	N.D.
Physics	$f_b$ : Respiratory frequency (rest)	-1/4	53.5 min <sup>-1</sup> [34]
	$V_T$ : Tidal volume (rest)	1	7.69 mL [34]
	$P_{50}$ : $O_2$ affinity of blood	-1/12	37.05 mmHg*
	$R$ : Total resistance	-3/4	24.4 cmH <sub>2</sub> O s L <sup>-1</sup> [34]
	$C$ : Total compliance	1	1.56 mL cmH <sub>2</sub> O <sup>-1</sup> [34]
	$P_{pl}$ : Interpleural pressure	0	N.D.
Variables	Exponent at BMR	Exponent at FMR	Exponent at MMR
$\dot{V}_{O_2}$ : $O_2$ consumption rate	3/4 [20, 29]	0.64 [16]	7/8 [39]
$t_c$ : Transit time of blood in pulmonary capillaries	1/4 [13, 40]	1/4 (hypothesized)	0.165 [4, 13]

TABLE I. Predicted and observed/computed values of allometric exponents for variables of the mammalian respiratory system. \*: Prefactor computed using human values ( $M = 70$  kg) at rest. BMR: Basal Metabolic Rate, FMR: Field Metabolic Rate, MMR: Maximal Metabolic Rate. N.D.: No data found.

the animal. It is assumed that the number of generations of alveolar ducts in the acinus is independent on the mass [12, 30]. Consequently  $\rho_s$  is also independent on the mass in our model. Under these conditions, the amount of exchange surface in our model fits the allometric law  $S_A \propto M^{11/12}$ .

### Oxygen and carbon dioxide transport and capture

The transport of oxygen and carbon dioxide in the lung is driven by three phenomena: convection by the airflow, diffusion and exchange with blood through the alveoli walls.

The mean partial pressure of oxygen over the section of a bronchus is transported along the longitudinal axis  $x$  of the bronchus. In the alveolar ducts in the acini, the additional phenomena of exchange with blood occurs. It can be represented with a reactive term based on a reactive constant  $\beta$  that accounts for the capture of oxygen by the duct wall.

Hence, in each bronchus of the lung belonging to generation  $i$ , the partial pressure of the respiratory gas follows

the transport equation

$$\frac{\partial P_i}{\partial t} - \underbrace{D \frac{\partial^2 P_i}{\partial x^2}}_{\text{diffusion}} - \underbrace{u_i(t) \frac{\partial P_i}{\partial x}}_{\text{convection}} + \underbrace{\beta_i (P_i - P_{\text{blood}})}_{\text{exchange with blood}} = 0, \quad \text{for } x \in [0, l_i], \quad (2)$$

where  $P_i$  is the mean partial pressure of the gas (mmHg) along the axis  $x$  of the bronchus,  $D$  is the diffusion coefficient in air of the gas considered and  $u_i(t)$  is the air velocity in the bronchus of generation  $i$ . The reactive term  $\beta_i$  that mimics the exchanges with the blood through the bronchi wall is equal to zero in the convective tree ( $i = 0 \dots G$ ) and positive in the acini ( $i = G + 1 \dots N$ ). A value of  $\beta_i$  different from zero means that gas exchanges occur through the wall of the duct, with the gas crossing the alveolar–capillary membrane whose thickness can be considered as mass independent,  $\tau \simeq 1 \mu\text{m}$  [31]. Assuming that the diffusivity of the gas in the tissues can be approximated with the diffusivity in water [31], the flow rate of the gas partial pressure per unit length of the bronchus is

$$\begin{aligned} \beta_i (P_i - P_{\text{blood}}) &= \rho_s \frac{2\pi r_i}{\pi r_i^2} k \sigma_{\text{gas, H}_2\text{O}} \frac{D_{\text{gas, H}_2\text{O}}}{\tau} (P_i - P_{\text{blood}}) \\ &= \rho_s \frac{2k}{r_i} \alpha (P_i - P_{\text{blood}}), \end{aligned}$$

where  $k$  is the ratio relating partial pressure of the gas to its concentration in water,  $\sigma_{\text{gas, H}_2\text{O}}$  is the solubility coefficient of the gas in water and  $D_{\text{gas, H}_2\text{O}}$  is the

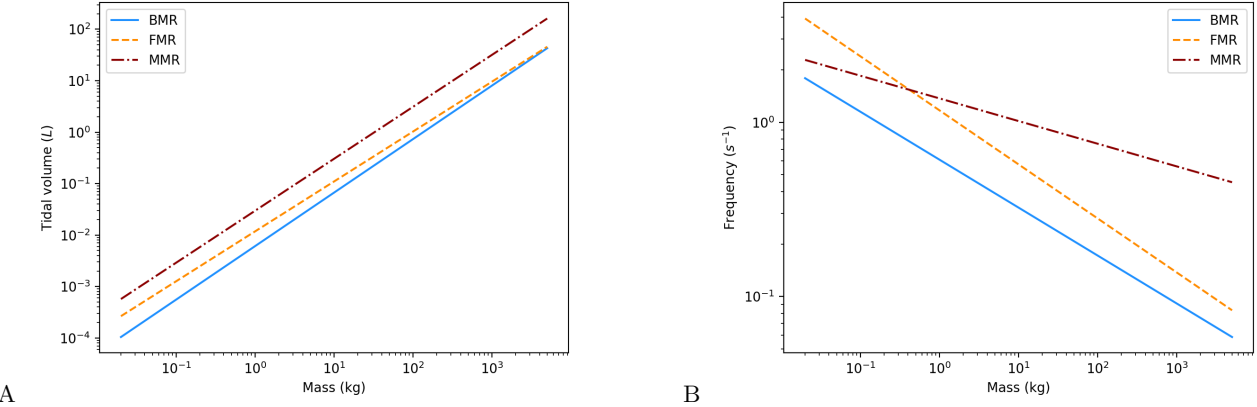


FIG. 1. **A:** Predicted tidal volume as a function of the mammals' mass (log-log). Solid line: BMR,  $V_T^{\text{BMR}} \simeq 6.1 M^{1.04}$  ml; dashed line: FMR,  $V_T^{\text{FMR}} \simeq 11.8 M^{0.97}$  ml, dash-dotted line: MMR,  $V_T^{\text{MMR}} \simeq 29.7 M^{1.01}$  ml. **B:** Predicted breathing frequency as a function of the mammals' mass (log-log). Solid line: BMR,  $f_b^{\text{BMR}} \simeq 0.61 M^{-0.27}$  Hz; dashed line: FMR,  $f_b^{\text{FMR}} \simeq 1.17 M^{-0.31}$  Hz, dash-dotted line: MMR,  $f_b^{\text{MMR}} \simeq 1.37 M^{-0.17}$  Hz. The crossing of FMR and MMR curves predicted by our model is due to the increase of bronchi diameter at higher regimes extrapolated from humans [13] to all mammals.

diffusion coefficient of the gas in water. The permeability of the alveolar membrane  $\alpha$  is defined as follow,  $\alpha = \sigma_{\text{gas}, \text{H}_2\text{O}} \frac{D_{\text{gas}, \text{H}_2\text{O}}}{\tau}$ .

Partial pressures continuity and mass conservation are assumed in the bifurcations. To determine the oxygen partial pressure in the blood plasma that drives the exchange, we assume that the flow of oxygen leaving the alveolar duct through its wall is equal to the flow of oxygen that is captured by the blood, accounting for the oxygen dissolved in the plasma and for the oxygen captured by the haemoglobin [8, 27].

Finally, we evaluate the flow of oxygen exchanged with the blood using

$$f_{O_2}(U, T) = \sum_{i=G+1}^N 2^i \int_{t_C}^{t_C+T} \int_0^{l_i} \beta_i (P_i(x) - P_{\text{blood}}(x)) dx$$

with  $t_C$  a time at which the system has reached a periodic regime.

## RESULTS

### Allometric scaling laws of breathing rates and tidal volumes

In 1950, Otis et al. showed that by constraining the alveolar ventilation  $\dot{V}_A = (V_T - V_D)f_b$  within  $\mathcal{P}(V_T, f_b)$  with  $V_D$  the dead volume, an optimal breathing frequency could be computed analytically by canceling the derivative of the power relatively to  $f_b$  [18, 28],

$$f_{b,\text{pred}} = \frac{2\dot{V}_A/V_D}{1 + \sqrt{1 + 4\pi^2 R C \dot{V}_A/V_D}}.$$

At BMR, the allometric scaling laws of all the physiological quantities involved in this expression for  $f_b$  are available in the literature:  $\dot{V}_A \propto M^{\frac{3}{4}}$  [10],  $V_D \propto M^1$  [34],  $R \propto M^{-\frac{3}{4}}$  [34, 40] and  $C \propto M^1$  [34]. Hence we are able to derive an allometric scaling law for breathing rate at BMR,  $f_b^{\text{BMR}}$ , based on ventilation data in healthy young humans [13],  $f_{b,\text{pred}}^{\text{BMR}} \propto 0.9 M^{-\frac{1}{4}}$  Hz. From the breathing frequency and still based on ventilation data from [13], we can deduce the allometric scaling law for the tidal volume at BMR,  $V_T^{\text{BMR}} = \dot{V}_A/f_b^{\text{BMR}} + V_D$ . Since  $\dot{V}_A/f_b^{\text{BMR}} \propto M^{\frac{3}{4}}/M^{-\frac{1}{4}}$  and  $V_D \propto M^1$ , we have  $V_{T,\text{pred}}^{\text{BMR}} = 7.5 M^1$  ml. However, this approach is not able to predict the allometric laws at other regimes than BMR. As the localization of the convection–diffusion transition zone guides the blood–gas exchange, which has to be adapted to the metabolic needs, the localization and the refresh rate of the transition zone have to be tuned depending on the regime. These properties depend on the morphology of the lung that has to be accounted for in order to be able to reach predictions whatever the regime.

Our analysis explores a set of masses ranging from the mouse (20 grams) to the elephant (5 tons) under three regimes: basal metabolic rate (BMR), field metabolic rate (FMR) and maximal metabolic rate (MMR). The power  $\mathcal{P}(U, T)$  is optimized with the constraint  $f_{O_2}(U, T) = \dot{V}_{O_2}$ . Both predicted breathing rates and tidal volumes under the three regimes follow allo-

metric scaling laws, as shown in Figure 1.

At  $\dot{V}_{O_2}^{\text{BMR}}$ :

$$f_b^{\text{BMR}} \simeq 0.61 M^{-0.27} \text{ Hz}, \quad V_T^{\text{BMR}} \simeq 6.1 M^{1.04} \text{ ml}$$

at  $\dot{V}_{O_2}^{\text{FMR}}$ :

$$f_b^{\text{FMR}} \simeq 1.17 M^{-0.31} \text{ Hz}, \quad V_T^{\text{FMR}} \simeq 11.8 M^{0.97} \text{ ml}$$

at  $\dot{V}_{O_2}^{\text{max}}$ :

$$f_b^{\text{MMR}} \simeq 1.37 M^{-0.17} \text{ Hz}, \quad V_T^{\text{MMR}} \simeq 29.7 M^{1.01} \text{ ml}$$

These results are only slightly sensitive to the allometric scaling law of the blood residence time in the pulmonary capillaries. The hydrodynamic resistance  $R$  is positively correlated to the exponent of the breathing rate  $f_b$ . A hydrodynamic resistance independent on the ventilation regime leads to good predictions for the breathing rate at both BMR and MMR. If we neglect the increased inertia and turbulence in the bronchi at MMR, the change in dead volume at this regime leads the hydrodynamic resistance to be decreased by a factor larger than 3. In this case, the corresponding exponent for breathing rate drops to  $-0.10$ . Consequently inertia and turbulence might play an important role on the control of breathing rate, but, interestingly, their influence seems to be balanced by the increase of the dead volume.

### Transition between convection and diffusion

The localization of the transition between convective and diffusive transports can be estimated by the analysis of the variations with the mass of the Péclet number, through the generations. This number arises by writing the transport equations in their dimensionless form. From Eq. 2,

$$\frac{2l_i^2}{DT} \frac{\partial P_i}{\partial s} - \frac{\partial^2 P_i}{\partial \xi^2} + \underbrace{\frac{l_i u_i (sT/2)}{D}}_{\text{Pe}_i(s)} \frac{\partial P_i}{\partial \xi} + \frac{\beta_i l_i^2}{D} (P_i - P_{\text{blood}}) = 0, \quad \text{for } \xi \in [0, 1]. \quad (3)$$

The dimensionless time is  $s = 2t/T$  with  $T/2$  the inspiration or expiration time and the dimensionless space is  $\xi = x/l_i$ . The mean Péclet number over a half breath is then  $\text{Pe}_i = \frac{2V_T f_b l_0}{\pi r_0^2 D} \left(\frac{1}{2h}\right)^i$ . The localization of the transition zone is reached when  $\text{Pe}_i$  becomes smaller than one over the ventilation cycle. This transition occurs at the generation  $k$ , with  $k$  such that

$$2^k = \left(\frac{2V_T f_b l_0}{\pi r_0^2 D}\right)^{\frac{3}{2}} = \left(2\dot{V}_E \frac{l_0}{\pi r_0^2 D}\right)^{\frac{3}{2}} \propto \dot{V}_E^{\frac{3}{2}} \times M^{-\frac{3}{4}}$$

At rest, the resulting allometric scaling law on the localization of the transition zone between convection and diffusion is  $2^{k_r} \propto M^{0.375}$ . At exercise, the scaling predicted

by our model is different with  $2^{k_e} \propto M^{0.6}$ . Hence, the transition generation  $k$  can be localized relatively to the generation of the terminal bronchioles  $G$  at both regimes:

$$k_r = G + 2.64 - 0.5 \log(M) / \log(2);$$

$$k_e = G + 6.67 - 0.275 \log(M) / \log(2).$$

At exercise, the transition occurs deeper in the lung of

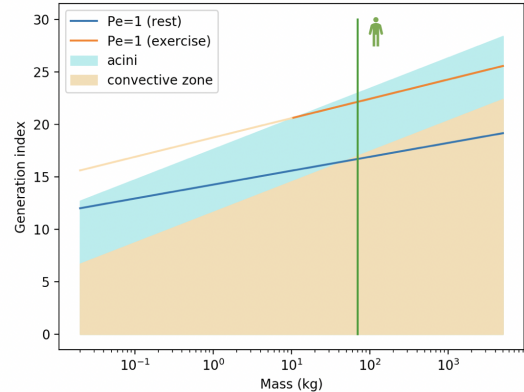


FIG. 2. Localization of the transition between a convective and diffusive transport of the oxygen in the lung as a function of the animal's mass (logarithmic scale). The lines correspond to the localizations of that transition at BMR (rest, blue line) and MMR ( $\dot{V}_{O_2}^{\text{max}}$ , orange line). The vertical green line corresponds to human's mass (70 kg). The lower beige region corresponds to the convective zone of the lung, while the upper blue region corresponds to the exchange surface (acini). Small mammals tend to transport oxygen mainly by convection and to use efficiently their exchange surface at rest, with the drawback to have few reserve for increasing their metabolic rate. To the contrary, due to the screening effect [31], large mammals use only a small portion of their exchange surface at rest. Hence, large mammals have large reserve of exchange surface available for higher metabolic rates.

mammals than at rest. Animals with lower mass have a transition which occurs relatively deeper in their lung, as shown in Figure 2. In the acini, the oxygen is simultaneously motioned along the alveolar ducts and captured by the blood flowing in the alveoli walls. Consequently, the first alveolar ducts get higher oxygen concentration than those deeper. This phenomenon is known as the screening effect [31] and results in an exchange surface that can be only partly active, depending on the localization in the lung of the transition between convection and diffusion. Our model predicts that small mammals are using almost all the volume of their lungs at rest, with low screening effect. To the contrary, large mammals present a clear difference in term of volume usage between rest and exercise, with a transition localized near the end of the bronchial tree at rest, with strong screening effect, and a transition localized deeper in the acini at exercise, with a lower screening effect.

### Exhaled oxygen fraction

The oxygen flow captured by the lung is a proportion of the air flow inhaled,  $\dot{V}_{O_2} = \dot{V}_E (f_I - f_E)$  with  $\dot{V}_E = V_T f_b$  the air flow rate,  $f_I$  the oxygen fraction in ambient air and  $f_E$  the mean exhaled oxygen fraction. The allometric laws predicted by our model for tidal volumes and breathing rates allow to derive similar laws for the drop in oxygen fraction between ambient and exhaled air,  $\Delta f = f_I - f_E$ :  $\Delta f^{\text{BMR}} = 4.61 M^{0.002} \%$ ,  $\Delta f^{\text{FMR}} = 5.02 M^{-0.009} \%$  and  $\Delta f^{\text{MMR}} = 5.12 M^{0.0005} \%$ . The drop in oxygen fraction depends only slightly on the mass and is in the range 3 to 5%, whatever the ventilation regime. With an inhaled oxygen fraction in air of about 21%, the oxygen fraction in the exhaled air is ranging from 16 to 18%, in full accordance with the physiology [38]. The quantity  $\eta = \Delta f / f_I$  can be considered as a measure for the efficiency of oxygen extraction by the lung. Our model suggests that the system extraction is optimal for values of  $\eta$  of about 20%. Differences in  $\eta$  exists between small and large mammals because of the non zero exponents in the allometric scaling laws of  $\Delta f$ . However, the values of these exponents are small and cannot be interpreted as such. They might be the results of the simplifications made in the model and/or of the numerical approximations.

## DISCUSSION

From a set of core morphometric parameters that represent the lung's geometry, our model allows to predict, at any metabolic regime, a set of dynamical parameters that represent the lung's ventilation and that minimize an estimation of the mechanical cost of ventilation. This approach is able to predict with good accuracy the allometric scaling laws of mammals' tidal volumes and breathing frequencies available in the literature (tidal volume at rest, breathing frequencies at rest and  $\dot{V}_{O_2}^{\text{max}}$  [2, 34, 40, 42, 43]). The validation of our model at both minimal and maximal metabolic regime suggests that its predictions are able to bring insights in the physiology of ventilation whatever the regime, in the limit of the availability of the input parameters. This suggests that the mechanical energy spent for ventilation might have driven the selection of ventilation patterns by evolution. The optimization process was functionally constrained, because the lung has to fulfil the function of transporting the needed respiratory gas to and from the blood. However, the function is dependent on the physical processes on which these transports rely. The most crucial physical phenomena is the screening effect [31]. Screening effect affects how the exchange surface is effectively used and drives at which depth in the lung the convection has to bring oxygen so that diffusion could take over the transport. The lung's response to change

in the metabolic regime is to adjust the amount of exchange surface effectively used. Hence, only an analysis including a reliable representation of the mammal's lung and of the gas transport is able to reach predictions compatible with the physiology, whatever the regime.

The idealized representation of the bronchial tree and of the exchange surface used in this study accounts for five core characteristics common to all the mammals' lungs, as identified in the literature [24, 27, 28, 38, 40]: a bifurcating tree structure; an homogeneous decrease of the size of the bronchi at the bifurcations; the size of the trachea; the size of the alveoli; and the surface area of the exchange surface. These characteristics are the main determinants of the tuning of ventilation in order to minimize the energetic cost of ventilation. This indicates that once the metabolic regime is fixed, the morphology of the lung is probably the primary driver of the physiological control of ventilation. We tested this hypothesis by altering in our analysis the allometric scaling laws related to the geometry of the lung. We observed corresponding alteration of the laws predicted for tidal volumes and breathing frequencies. Since morphology itself has probably been selected by evolution in order to minimize the hydrodynamic resistance in a constrained volume [24], morphology and ventilation patterns are intertwined together in order for the lung to function with a low global energetic cost, i.e. a low hydrodynamic resistance  $R$  and a low ventilation cost  $\hat{P}(V_T, f_b)$  that also depends on  $R$ . Interestingly, our representation of the lung does not account for interspecific differences known to exist between the lungs of mammals, such as different degrees of branching asymmetry, monopodial or bipodial lungs, etc. [9, 22, 26, 35]. Nevertheless, the predictions of our model for the localization of the convection–diffusion transition ( $\text{Pe} = 1$ ) in idealized lungs lead to good estimations of the allometric scaling laws for tidal volumes and breathing frequencies, indicating that the morphological parameters included in our model might primarily drive the control of ventilation.

The generation index of the convection–diffusion transition, shown in Figure 2, depends linearly on the logarithm of the mass. Since the structure of the tree is also governed by allometric scaling laws, the generation index at which the transition between the bronchial tree and the acini occurs also depends linearly on the logarithm of the mass of the animal. However, the slopes are different and the convection–diffusion transition is located in the acini for small mammals and in the lower bronchial tree for large mammals. The reason is that larger mammals actually need less oxygen relatively to their mass than small mammals, as  $\dot{V}_{O_2}/M \propto M^{-1/4}$  at rest and  $\dot{V}_{O_2}^{\text{max}}/M \propto M^{-1/8}$  at  $\dot{V}_{O_2}^{\text{max}}$ . Hence, at rest, small mammals use a large portion of their exchange surface, while large mammals tends to use a small portion of that surface. This suggests that large mammals have more reserve to increase their

metabolic rates, in the limit of other physiological constraints, such as their ability to dissipate the excess of heat [32, 33]. Interestingly, for masses near that of a human, the convection–diffusion transition occur near the beginning of the acini [19, 27, 31].

The ability to increase the metabolic rates plays a crucial role in animal life, for example for foraging or for responding to environmental threat. Our model suggests that the proportion of oxygen extracted from the ambient air by the lung, found to be about 20%, depends only slightly on the metabolic regime. More oxygen is extracted at higher metabolic regimes because the volumes of air inhaled are larger. A larger volume of air inhaled allows to use a larger portion of the exchange surface, hence reducing *de facto* the screening effect and accelerating the exchange speed. As a consequence, air has to be renewed at a quicker pace and breathing rate is increased. This effect is however counterbalanced by the increase of the dead volume during exercise [5]. A larger dead volume allows to optimize the mechanical energy with a breathing rate that is lower than it would be for a rest dead volume. In particular, our model suggests that this effect is predominant on the control of breathing rates in small mammals. Since small mammals already use most of their exchange surface at BMR, they have almost no margin for increasing the available surface at exercise. However, the hypothesized larger dead volume allows to bring a larger oxygen reserve at the convection–diffusion transition point. The balance between the increased volume and the air renewal rate needed to maintain an efficient diffusion gradient leads our model to predict for small mammals a breathing rate at MMR smaller than at FMR, as shown in Figure 1. A more detailed analysis of the trade-off is however needed to confirm or infirm this trend.

## CONCLUSION

Our results highlight how the transport of the respiratory gas influences the control of ventilation, and more generally, the behavior of the lung and respiratory system. Our results contribute to improve our understanding of the allometric scaling of ventilation in mammals. They represent a new theoretical framework explaining how the evolution might have driven the design of the respiratory system and its links with the organism’s metabolism. Our work suggests that the dynamical characteristics related to the control of ventilation is highly dependent on the morphological characteristics of the lung. This dependence comes from the physical processes involved in oxygen transport. Moreover, it has been suggested that several core morphological parameters related to the bronchial tree minimize the hydrodynamic resistance of the lung in a limited volume, so that the exchange surface can fill most of the thoracic

space [24]. Consequently, the control of ventilation is, at least partially, a direct consequence of the repartition of lung’s space between the bronchial tree and the acini. More generally, this highlights the importance of the geometrical constraints in the selection of organs’ characteristics, not only in terms of morphology, but also in terms of dynamics.

---

- [1] V. Agostini, E. Chiaramello, C. Bredariol, C. Cavallini, and M. Knaflitz. Postural control after traumatic brain injury in patients with neuro-ophthalmic deficits. *Gait & Posture*, 34(2):248–253, June 2011.
- [2] J. D. Altringham and I. S. Young. Power output and the frequency of oscillatory work in mammalian diaphragm muscle: the effects of animal size. *Journal of Experimental Biology*, 157(1):381–389, May 1991.
- [3] J. Bezanson, A. Edelman, S. Karpinski, and V. B. Shah. Julia: A fresh approach to numerical computing. *SIAM review*, 59(1):65–98, 2017. Publisher: SIAM.
- [4] C. M. Bishop and R. J. Spivey. Integration of exercise response and allometric scaling in endotherms. *Journal of Theoretical Biology*, 323:11–19, Apr. 2013.
- [5] J. A. Dempsey and A. J. Jacques. Respiratory System Response to Exercise in Health. In M. A. Grippi, J. A. Elias, J. A. Fishman, R. M. Kotloff, A. I. Pack, R. M. Senior, and M. D. Siegel, editors, *Fishman’s Pulmonary Diseases and Disorders*. McGraw-Hill Education, New York, NY, 5 edition, 2015.
- [6] D. S. Dhindsa, A. S. Hoversland, and J. Metcalfe. Comparative studies of the respiratory functions of mammalian blood. VII. Armadillo (*Dasypus novemcinctus*). *Respiration Physiology*, 13(2):198–208, Nov. 1971.
- [7] D. Elad, R. D. Kamm, and A. H. Shapiro. Steady compressible flow in collapsible tubes: application to forced expiration. *Journal of Fluid Mechanics*, 203:401–418, June 1989.
- [8] M. Felici. *Physics of the oxygen diffusion in the human lung*. PhD thesis, Ecole Polytechnique X, June 2003.
- [9] M. Florens, B. Sapoval, and M. Filoche. Optimal Branching Asymmetry of Hydrodynamic Pulsatile Trees. *Physical Review Letters*, 106(17):178104, Apr. 2011.
- [10] B. Gunther. Dimensional analysis and theory of biological similarity. *Physiological Reviews*, 55(4):659–699, Oct. 1975.
- [11] B. Günther and B. L. De la Barra. Physiometry of the mammalian circulatory system. *Acta Physiologica Latino Americana*, 16(1):32–42, 1966.
- [12] B. Haefeli-Bleuer and E. R. Weibel. Morphometry of the human pulmonary acinus. *The Anatomical Record*, 220(4):401–414, Apr. 1988.
- [13] H. C. Haverkamp, J. A. Dempsey, J. D. Miller, L. M. Romer, and M. W. Eldridge. Physiologic responses to exercise. In *Physiologic basis of respiratory disease*, page 17. BC Decker, Inc, Hamilton, 2005.
- [14] R. Hill, H. P. Wolvokamp, and F. G. Hopkins. The oxygen dissociation curve of haemoglobin in dilute solution. *Proc. R. Soc. Lond. B*, 120(819):484–495, 1936.
- [15] C. C. Hsia, D. M. Hyde, and E. R. Weibel. Lung Structure and the Intrinsic Challenges of Gas Exchange.

In R. Terjung, editor, *Comprehensive Physiology*, pages 827–895. John Wiley & Sons, Inc., Hoboken, NJ, USA, Mar. 2016.

[16] L. N. Hudson, N. J. B. Isaac, and D. C. Reuman. The relationship between body mass and field metabolic rate among individual birds and mammals. *Journal of Animal Ecology*, 82(5):1009–1020, 2013. [eprint: https://besjournals.onlinelibrary.wiley.com/doi/pdf/10.1111/2656.12086](https://besjournals.onlinelibrary.wiley.com/doi/pdf/10.1111/2656.12086).

[17] J. S. Huxley and G. Teissier. Terminology of Relative Growth. *Nature*, 137(3471):780–781, May 1936.

[18] A. T. Johnson. *Biomechanics and Exercise Physiology: Quantitative Modeling*. CRC Press, Mar. 2007. Google-Books-ID: oIvMBQAAQBAJ.

[19] C. Karamaoun, B. Sobac, B. Mauroy, A. V. Muylem, and B. Haut. New insights into the mechanisms controlling the bronchial mucus balance. *PLOS ONE*, 13(6):e0199319, June 2018.

[20] M. Kleiber. Body size and metabolism. *Hilgardia*, 6(11):315–353, Jan. 1932.

[21] B. Mauroy. *Viscosity : an architect for the respiratory system?* Habilitation à diriger des recherches, Université de Nice-Sophia Antipolis, Dec. 2014.

[22] B. Mauroy and P. Bokov. The influence of variability on the optimal shape of an airway tree branching asymmetrically. *Physical Biology*, 7(1):16007, 2010.

[23] B. Mauroy, M. Filoche, J. S. Andrade, and B. Sapoval. Interplay between geometry and flow distribution in an airway tree. *Physical Review Letters*, 90(14):148101, Apr. 2003.

[24] B. Mauroy, M. Filoche, E. R. Weibel, and B. Sapoval. An optimal bronchial tree may be dangerous. *Nature*, 427(6975):633–636, Feb. 2004.

[25] J. Mead. Control of respiratory frequency. *Journal of Applied Physiology*, 15(3):325–336, May 1960.

[26] A. Monteiro and R. L. Smith. Bronchial tree Architecture in Mammals of Diverse Body Mass. *International Journal of Morphology*, 32(1):312–316, Mar. 2014.

[27] F. Noël and B. Mauroy. Interplay Between Optimal Ventilation and Gas Transport in a Model of the Human Lung. *Frontiers in Physiology*, 10, 2019.

[28] A. B. Otis, W. O. Fenn, and H. Rahn. Mechanics of Breathing in Man. *Journal of Applied Physiology*, 2(11):592–607, May 1950.

[29] R. H. Peters. *The ecological implications of body size*, volume 2. Cambridge University Press, 1986.

[30] M. Rodriguez, S. Bur, A. Favre, and E. R. Weibel. Pulmonary acinus: Geometry and morphometry of the peripheral airway system in rat and rabbit. *American Journal of Anatomy*, 180(2):143–155, 1987.

[31] B. Sapoval, M. Filoche, and E. R. Weibel. Smaller is better—but not too small: A physical scale for the design of the mammalian pulmonary acinus. *Proceedings of the National Academy of Sciences*, 99(16):10411–10416, June 2002.

[32] B. Sobac, C. Karamaoun, B. Haut, and B. Mauroy. Allometric scaling of heat and water exchanges in the mammals' lung. *arXiv:1911.11700 [physics]*, Dec. 2019. arXiv: 1911.11700.

[33] J. R. Speakman and E. Król. The Heat Dissipation Limit Theory and Evolution of Life Histories in Endotherms—Time to Dispose of the Disposable Soma Theory? *Integrative and Comparative Biology*, 50(5):793–807, Nov. 2010.

[34] W. R. Stahl. Scaling of respiratory variables in mammals. *J. appl. Physiol*, 22(3):453–460, 1967.

[35] M. H. Tawhai, P. Hunter, J. Tscherren, J. Reinhardt, G. McLennan, and E. A. Hoffman. CT-based geometry analysis and finite element models of the human and ovine bronchial tree. *Journal of Applied Physiology (Bethesda, Md.: 1985)*, 97(6):2310–2321, Dec. 2004.

[36] S. M. Tenney and D. Bartlett. Comparative quantitative morphology of the mammalian lung: Trachea. *Respiration Physiology*, 3(2):130–135, Oct. 1967.

[37] S. M. Tenney and J. B. Tenney. Quantitative morphology of cold-blooded lungs: Amphibia and reptilia. *Respiration Physiology*, 9(2):197–215, May 1970.

[38] E. R. Weibel. *The Pathway for Oxygen: Structure and Function in the Mammalian Respiratory System*. Harvard University Press, 1984.

[39] E. R. Weibel and H. Hoppeler. Exercise-induced maximal metabolic rate scales with muscle aerobic capacity. *Journal of Experimental Biology*, 208(9):1635–1644, May 2005.

[40] G. B. West, J. H. Brown, and B. J. Enquist. A general model for the origin of allometric scaling laws in biology. *Science*, 276(5309):122–126, 1997.

[41] J. B. West. *Respiratory Physiology: The Essentials*. Lippincott Williams and Wilkins, Philadelphia, 9th revised edition edition, Aug. 2011.

[42] J. Worthington, I. S. Young, and J. D. Altringham. The relationship between body mass and ventilation rate in mammals. *Journal of Experimental Biology*, 161(1):533–536, Nov. 1991.

[43] I. S. Young, R. D. Warren, and J. D. Altringham. Some properties of the mammalian locomotory and respiratory systems in relation to body mass. *Journal of Experimental Biology*, 164(1):283–294, Mar. 1992.

## Boundary conditions

As the bronchi are connected through symmetrical dichotomous bifurcations, mass conservation over a bifurcation leads to

$$S_i \left( u_i(t) P_i(l_i, t) - D \frac{\partial P_i(l_i, t)}{\partial x} \right) - 2S_{i+1} \left( u_{i+1}(t) P_{i+1}(0, t) - D \frac{\partial P_{i+1}(0, t)}{\partial x} \right) = 0$$

Partial pressure continuity at bifurcations writes  $P_i(l_i, t) = P_{i+1}(0, t)$ . The mass conversation can be rewritten using continuity,

$$- DS_i \frac{\partial P_i(l_i, t)}{\partial x} = - 2DS_{i+1} \frac{\partial P_{i+1}(0, t)}{\partial x} \quad (4)$$

Boundary conditions and initial condition are expressed in order for the problem to be well-posed. We assume that  $P_0(0, t) = P_{\text{air}}$  at the trachea entrance, where  $P_{\text{air}}$  is the partial pressure of the respiratory gas in the air. At the bottom end of the tree, the gas exchange with blood is neglected (*élaborer cette hypothèse*), which writes  $-D \frac{\partial P_N}{\partial x}(l_A, t) = 0$ .

### Blood partial pressures

The blood partial pressure  $P_{\text{blood}}$  of oxygen depends non linearly on the local value of  $P_i$ , as a result of a balance between the amount of gas exchanged through the alveolo-capillary membrane and the amount of gas stored or freed during the passage of blood in the capillary [27].

As oxygen is stored within haemoglobin and dissolved in plasma, this balance writes

$$\alpha (P_{O_2} - P_{\text{blood},O_2}) = 4Z_0(f(P_{\text{blood},O_2}) - f(P_{aO_2})) + \sigma_{O_2} v_s (P_{\text{blood},O_2} - P_{aO_2}),$$

with  $Z_0$  the haemoglobin concentration, each of these molecules containing four sites of binding with oxygen molecules. The function  $f(x) = x^{2.6}/(x^{2.6} + 26^{2.6})$  is the Hill's equation [14] that reproduces the saturation of haemoglobin depending on the partial pressure of oxygen in blood. The quantity  $v_s$  corresponds to blood velocity in the capillaries and  $\sigma_{O_2}$  corresponds to the solubility coefficient of oxygen in blood. The pressure  $P_{aO_2}$  is the partial pressure of oxygen in the arterial lung's circulation (low oxygenated blood).

Blood mean velocity  $v_s$  depends on the mass and on the metabolic regime studied. It can be computed as the ratio of the length of the capillary  $l_c$  over the transit time in the capillary  $t_c$ . As in [40], we assume that the terminal units of the blood network are invariant in size. Hence, the capillary length is fixed constant in our model and equal to 1 mm. The transit time in capillaries depends both on the mass and on the metabolic regime,

$$t_c \simeq 0.36 M^{\frac{1}{4}} \quad \text{at basal metabolic rate [13, 40]}$$

$$t_c \simeq 0.25 M^{0.165} \quad \text{at maximal metabolic rate [4, 13]}$$

No data is available in the literature for the field

metabolic rate, so we derive the human value  $t_c = 838$  s using data from Haverkamp et al. [13]. Since the allometric laws for the field metabolic rate are very similar to the ones of the basal metabolic rate we take the same exponent. The allometric law for the transit time is deduced,

$$t_c \simeq 0.29 M^{\frac{1}{4}} \quad \text{at field metabolic rate}.$$

### Initial conditions

At time  $t = 0$ , we assume  $u_i(0) = 0$ ,  $\frac{\partial P_i}{\partial t}(0) = 0$  in the convective part of the tree and  $P_i$  constant in the acini. Then, an explicit stationary solution in the bronchial tree can be derived and used as a non trivial initial condition, for  $i = 1 \dots G$  with a value for  $P_{\text{blood}}$  fixed,

$$P_i(x) = P_{\text{air}} + \frac{P_{\text{blood}} - P_{\text{air}}}{\sum_{k=0}^N \left(\frac{1}{2h}\right)^k} \left( \sum_{k=0}^{i-1} \left(\frac{1}{2h}\right)^k + \left(\frac{1}{2h}\right)^i \frac{x}{l_i} \right).$$

For  $i = G + 1 \dots N$ , we suppose that the partial pressure is the same as the one in the blood,

$$P_i(x) = P_{\text{blood}}.$$

### Numerical scheme

This model is analyzed using numerical simulations to solve the system of equations. The numerical method is based on a discretization of the transport equations using an implicit finite differences scheme. The computation are performed using the computing language Julia [3]. From this initial distribution of partial pressures in the tree, the simulations are then run up to a time when the ventilation pattern becomes periodic in time.